The gut microbiota modulates host energy and lipid metabolism in mice[s]

Vidya R. Velagapudi,* Rahil Hezaveh,[†,§] Christopher S. Reigstad,[†,§] Peddinti Gopalacharyulu,* Laxman Yetukuri,* Sama Islam,[†,§] Jenny Felin,[†,§] Rosie Perkins,[†,§] Jan Borén,[†,§] Matej Orešič,*'** and Fredrik Bäckhed[1,†,§]

VTT Technical Research Centre of Finland,* Espoo, FI-02044 VTT, Finland; Sahlgrenska Center for Cardiovascular and Metabolic Research/Wallenberg Laboratory,[†] and Department of Molecular and Clinical Medicine,[§] University of Gothenburg, SE-413 45 Gothenburg, Sweden; and Institute of Molecular Medicine Finland FIMM,** Helsinki, FI-00014 University of Helsinki, Finland

Abstract   The gut microbiota has recently been identified as an environmental factor that may promote metabolic diseases. To investigate the effect of gut microbiota on host energy and lipid metabolism, we compared the serum metabolome and the lipidomes of serum, adipose tissue, and liver of conventionally raised (CONV-R) and germ-free mice. The serum metabolome of CONV-R mice was characterized by increased levels of energy metabolites, e.g., pyruvic acid, citric acid, fumaric acid, and malic acid, while levels of cholesterol and fatty acids were reduced. We also showed that the microbiota modified a number of lipid species in the serum, adipose tissue, and liver, with its greatest effect on triglyceride and phosphatidylcholine species. Triglyceride levels were lower in serum but higher in adipose tissue and liver of CONV-R mice, consistent with increased lipid clearance. Our findings show that the gut microbiota affects both host energy and lipid metabolism and highlights its role in the development of metabolic diseases.— Velagapudi, V.R., R. Hezaveh, C. S. Reigstad, P. Gopalacharyulu, L. Yetukuri, S. Islam, J. Felin, R. Perkins, J. Borén, M. Orešič, and F. Bäckhed. **The gut microbiota modulates host energy and lipid metabolism in mice.** *J. Lipid Res.* 2010. **51: 1101–1112.**

Supplementary key words   metabolomics • lipidomics

The mammalian gut microbiota is a complex and dynamic ecosystem (1–4) that has coevolved with its host (5). It has developed metabolic traits that complement the host's metabolism (6–8) and can thus be regarded as a metabolically active organ located within the mammalian gastrointestinal tract (9, 10). Studies comparing ileal tissue from germ-free (GF) and *Bacteroidetes thetaiotaomicron*-colonized mice have shown that microbial colonization modifies the expression of genes involved in the metabolism of xenobiotics (foreign compounds) as well as in host nutrient (amino acids, lipids, vitamins, and ions) absorption and processing (6).

Evidence is now accumulating to indicate that perturbations of gut microbiota composition/functions may play an important role in the development of diseases associated with altered metabolism (11, 12). The diversity of the gut microbiota in both mice and humans is low on the phylum level, where the majority of species (>95%) belong to Firmicutes and Bacteroidetes (1, 2, 13). In contrast, the microbial diversity on species levels is very high (1, 2, 13). Recent studies in both mice and humans demonstrated that obesity is associated with an altered gut microbial ecology, exemplified by lower microbial diversity and decreased levels of Bacteroidetes (2, 3, 13, 14). The shift in microbial composition is associated with alterations in the gut microbial metagenome, notably an enrichment of genes involved in energy harvest (15). Furthermore, GF mice have decreased adiposity and hepatic triglyceride levels compared with conventionally raised (CONV-R) mice and are resistant to diet-induced obesity (16, 17). Although the mechanisms through which the gut microbiota promotes obesity have not been clarified in detail, it is known

that GF mice have increased fatty acid oxidation and decreased lipogenesis (16, 17).

Novel approaches are now emerging to measure and model metabolism. A powerful approach to understand host metabolism is to produce multivariate phenotypic signatures such as metabolite profiles (metabolomics). Metabolomics of plasma from GF and CONV-R mice have begun to reveal a profound microbial effect of host metabolism, especially on amino acid metabolites (18, 19). For example, the gut microbiota is required for the production of bioactive indole-containing metabolites, such as the antioxidant indole-3-propionic acid, from tryptophan (19). Despite our increased understanding of how microbes affect the host metabolome (8, 18–22), our knowledge of microbial modulation of host energy and lipid metabolism is limited. In particular, it is not clear how the gut microbiota affects the systemic lipid metabolism in metabolically important organs such as adipose tissue and liver. Given the complexity of systemic lipid metabolism (23), it is clear that a multi-tissue approach is needed to clarify these issues.

Here, we use MS-based metabolomics of serum in combination with MS-based lipidomics of serum, white adipose tissue, and liver of GF and CONV-R mice to delineate how the gut microbiota affects the host's energy and lipid metabolism. We show that the presence of a gut microbiota is reflected by increased levels of pyruvic acid and tricarboxylic acid metabolites in serum. Furthermore, we observed altered lipid metabolism in serum, white adipose tissue, and liver, with the most notable effects on triglyceride and phosphatidylcholine species.

MATERIALS AND METHODS

Animals

Male GF Swiss Webster mice (aged 12–14 weeks) were maintained in flexible plastic film isolators under a strict 12-h-light cycle (lights on at 06:00 h). Sterility was routinely confirmed by culturing and PCR analysis from feces using universal primers amplifying the 16S rRNA gene. Age-matched male CONV-R Swiss Webster mice were transferred to identical isolators at weaning. Both groups of mice were fed an autoclaved chow diet (Labdiet, St. Louis, MO) ad libitum unless otherwise stated. To produce conventionalized (CONV-D) mice, we conventionalized 12-week-old GF mice with gut microbiota from Swiss Webster donor mice as previously described (16). The study protocols were approved by the University of Gothenburg Animal Studies Committee.

Blood was collected from the vena cava under deep isoflurane anesthesia after a 4 h fast, unless otherwise stated, and the mice were subsequently euthanized by cervical dislocation. The liver and epididymal white adipose tissues were immediately removed and snap frozen in liquid nitrogen.

Metabolomic analyses using GC coupled to time-of-flight MS platform

Serum samples (30 µl) were combined with 10 µl of an internal standard, labeled palmitic acid (16:0-16,16,16d$_3$; 500 mg/l), and 400 µl of methanol, vortexed for 2 min, and incubated for 30 min at room temperature. The supernatant was separated by centrifugation at 5,590 g for 5 min at room temperature. The sample

was dried under constant flow of nitrogen. Twenty-five microliters of 2% methoxyamine hydrochloride in pyridine was added to the dried sample and incubated at 45°C for 1 h and then derivatized with 25 µl of N-methyl-N-(trimethylsilyl)-trifluoroacetamide by incubating at 45°C for 1 h. Five microliters of retention index standard mixture with five alkanes (400 mg/l) was added to the metabolite mixture. Sample order for analysis was established by randomization. The samples were analyzed on a Leco Pegasus 4D GC coupled to time-of-flight MS (GCxGC-ToF/MS) mass spectrometer with Agilent technologies 6890N GC and Combi PAL autosampler.

The metabolites were identified using an in-house reference compound library and by searching the reference mass spectral library. Mass spectra from the GCxGC-TOF/MS analysis were searched against the Palisade Complete Mass Spectral Library, 600K Edition (Palisade Mass Spectrometry, Ithaca, NY), which includes all spectra available from the NIST 2002 and Wiley registry collections and 150,000 other spectra. The matches to reference spectra are based on a weighted dot product of the two spectra, with higher m/z peaks having more weight than the lower. A similarity value is assigned between 0 and 999, with 999 being a perfect match and 750 generally considered as a reasonable match. We used the conservative cutoff criterion of 850 for identification.

Lipidomic analyses using ultra performance liquid chromatography/MS platform

Serum (10 µl) and liver samples (5–10 mg) were diluted with 0.9% NaCl (10 µl for serum, 50 µl for liver) and adipose tissue samples (5–10 mg) were diluted with 200 µl PBS buffer. All samples were spiked with an internal standard (10 µl for serum and liver, 20 µl for adipose) (24). The samples were subsequently extracted with chloroform-methanol (2:1) solvent (100 µl for serum, 200 µl for liver, 400 µl with 40 µl of PBS buffer for adipose), homogenized with a glass rod (serum) or a Retsch homogenizer (Mixer MILL type MM301) for 2 min at 25 Hz (liver) or 20 Hz (adipose) at 4°C by adding two zirconium oxide grinding balls, vortexed (1 min for serum, 2 min for liver and adipose), incubated at room temperature (1 h for serum and adipose, 30 min for liver), and centrifuged at 5,590 g for 3 min. From the separated lower phase, an aliquot (60 µl for serum, 100 µl for liver, 200 µl for adipose) was mixed with a labeled standard mixture (three stable isotope-labeled reference compounds; 10 µl for serum and liver, 20 µl for adipose) and 0.5–1.0 µl injection was used for LC/MS analysis. Sample order for analysis was established by randomization. Lipid extracts were analyzed on a Q-ToF Premier mass spectrometer (Waters) combined with an Acquity ultra performance liquid chromatography/MS (for specific settings, see Supplementary Methods).

Modeling

To include the correlation structure of lipidomics data into the analysis and therefore explore possible associations between different lipid molecular species, we applied the partial least squares discriminant analysis (PLS/DA) (25, 26) using the SIMPLS algorithm to calculate the model (27). PLS/DA is a common approach to multivariate metabolomics data analysis (28, 29). PLS/DA analysis maximizes the product of variance matrix of measured variables (e.g., lipidomic profile data) and correlation of measured data with properties of interest (e.g., CONV-R vs. GF mice). PLS/DA makes latent variables of original matrix X (predictor variable, e.g., lipidomics data) and matrix Y (response variable; e.g., mouse groups). Latent variables are formed as a linear combination of all the original variables in X in such a way that most of the association with Y variables can be explained together

with the variation in *X*. Contiguous-blocks cross-validation method and Q^2 scores were used to develop the models (30). Q^2 indicates how accurately the data, either classed or nonclassed, can be predicted, and this term is more relevant to supervised pattern recognition processes. Q^2 scores over 0.08 indicate a model that is better than chance, whereas a score between 0.7 and 1.0 demonstrates a highly robust trend. For each model built, the loading scores and the variable importance on projection (VIP) parameters were examined, in conjunction with the original data, to identify which metabolites contributed most to clusterings or a trend observed in the data. Loading scores describe the correlation between the original variables and the new component variables, whereas VIP parameters are essentially a measure of the degree to which a particular variable explains the *Y* variance (class membership). PLS/DA analyses were performed using Matlab, version 7.5 (Mathworks, Natick, MA) and PLS Toolbox, version 4.2, of the Matlab package (Eigenvector Research, Wenatchee, WA).

Measurements of serum lipids

Total serum triglycerides and cholesterol were analyzed according to the manufacturer's protocols (Thermo Electron, Grenoble, France). The lipid distribution in plasma lipoprotein fractions was assessed by fast protein liquid chromatography gel filtration with a Superose 6 HR 10/30 column (Pharmacia, Uppsala, Sweden). Each fraction was subsequently analyzed for triglyceride or cholesterol content as above. Plasma lipoproteins were also separated by agarose gel electrophoresis (31) and the chylomicron staining was quantified by densitometry.

Hepatic VLDL production

To determine the VLDL production rate, lipolysis was blocked by injecting mice with 12.5 mg of Triton WR1339 (10% solution in saline) intravenously after an overnight fast. Blood samples were drawn from the tail vein at 0, 10, 30, 60, and 90 min after injection. Triglycerides were measured using an enzymatic colorimetric assay (Thermo Electron, Grenoble, France) according to the manufacturer's protocol.

Administration of lipid bolus

Mice were gavaged with 400 µl heavy whipping cream (36% fat, Arla, Sweden) after an overnight fast and euthanized 1 or 4 h after the lipid bolus. Serum was collected and triglycerides were measured as above.

Statistics

Student's *t*-test was applied to test for pairwise differences between the means, single factor ANOVA was applied to test for differences among means, and Dunn-Sidák multiple comparison procedure was applied to identify which means were significantly different, using the *multcompare* function of the MATLAB Statistical Toolbox. *P* values < 0.05 were considered as statistically significant. False Discovery Rate or the expected proportion of false discoveries among the rejected hypotheses was estimated using the method by Benjamini et al. (32). The adjusted *P* values (*q* values) were calculated with the function "p.adjust" using the R statistical software (http://www.r-project.org/).

RESULTS

The gut microbiota affects the serum metabolome

We performed MS-based metabolic profiling of serum from CONV-R and GF Swiss Webster mice after a 4 h fast by using two-dimensional GC coupled to time-of-flight MS (GCxGC-ToF/MS) and identified 185 metabolites. Modeling and clustering by PLS/DA revealed that serum metabolite profiles clustered according to colonization status (**Fig. 1A**, corresponding VIP values are listed in supplementary Table I, and all 29 metabolites that are significantly altered in CONV-R compared with GF mice are listed in supplementary Table II).

As expected, we observed increased levels of the microbially derived metabolites and metabolites involved in xenobiotic metabolism in serum from CONV-R mice (Fig. 1B). 3-Hydroxyphenylpropionic acid, a product of catechin metabolism (33), and hydrocinnamic acid (or benzenepropanoic acid), which is produced by clostridium species (34), were elevated in CONV-R mice. In addition, we observed increases in rhamnose, a component of the outer cell membrane of acid-fast bacteria in the mycobacterium genus (35) (Fig. 1B). These findings demonstrate that the host serum metabolite profile reflects microbial metabolism in the intestine. Serum levels of glucuronic acid, which is associated with phase II (conjugation) metabolism of xenobiotic compounds (36), were also increased in CONV-R mice compared with CONV-R mice (Fig. 1B). This increase is consistent with increased expression of *Ugt2b38* in the liver (R. Hezaveh, C. Reigstad, P. Gopalacharyulu, M. Oresic, F. Bäckhed, unpublished data).

The gut microbiota also promoted increases in the serum levels of pyruvic acid and the tricarboxylic acid metabolites citric acid, fumaric acid, and mails acid (all metabolites involved in energy metabolism) and reduced serum levels of urea and the urea cycle metabolite L-ornithine (Fig. 1B). Serum levels of several essential cellular building blocks, including sugars, amino acids, and fatty acids, were also modified. In particular, serum from CONV-R mice had decreased levels of long-chain fatty acids [the saturated fatty acid palmitic acid (16:0) and the unsaturated essential fatty acid linoleic acid (18:2n-6)] and cholesterol, and increased levels of the dietary phytosterol campesterol and glucose (Fig. 1B). We also identified increased serum levels of the monoamine neurotransmitters dopamine and tyramine and of *trans*-2-aminomethylcyclopropanecarboxylic acid, a cyclopropane analog of γ-aminobutyric acid, in CONV-R mice (Fig. 1B).

The gut microbiota affects the serum lipidome

To investigate in further detail how the gut microbiota affects the serum lipidome, we performed high-resolution lipidomics of serum from CONV-R and GF mice after a 4 h fast using ultra performance liquid chromatography/MS. This technology allows several hundred lipid species to be simultaneously and accurately analyzed (24). We identified and quantified 333 lipids in serum from CONV-R and GF mice, and PLS/DA modeling and clustering revealed significant differences in the global serum lipid profiles between CONV-R and GF mice (**Fig. 2A**; corresponding VIP values are listed in supplementary Table III,
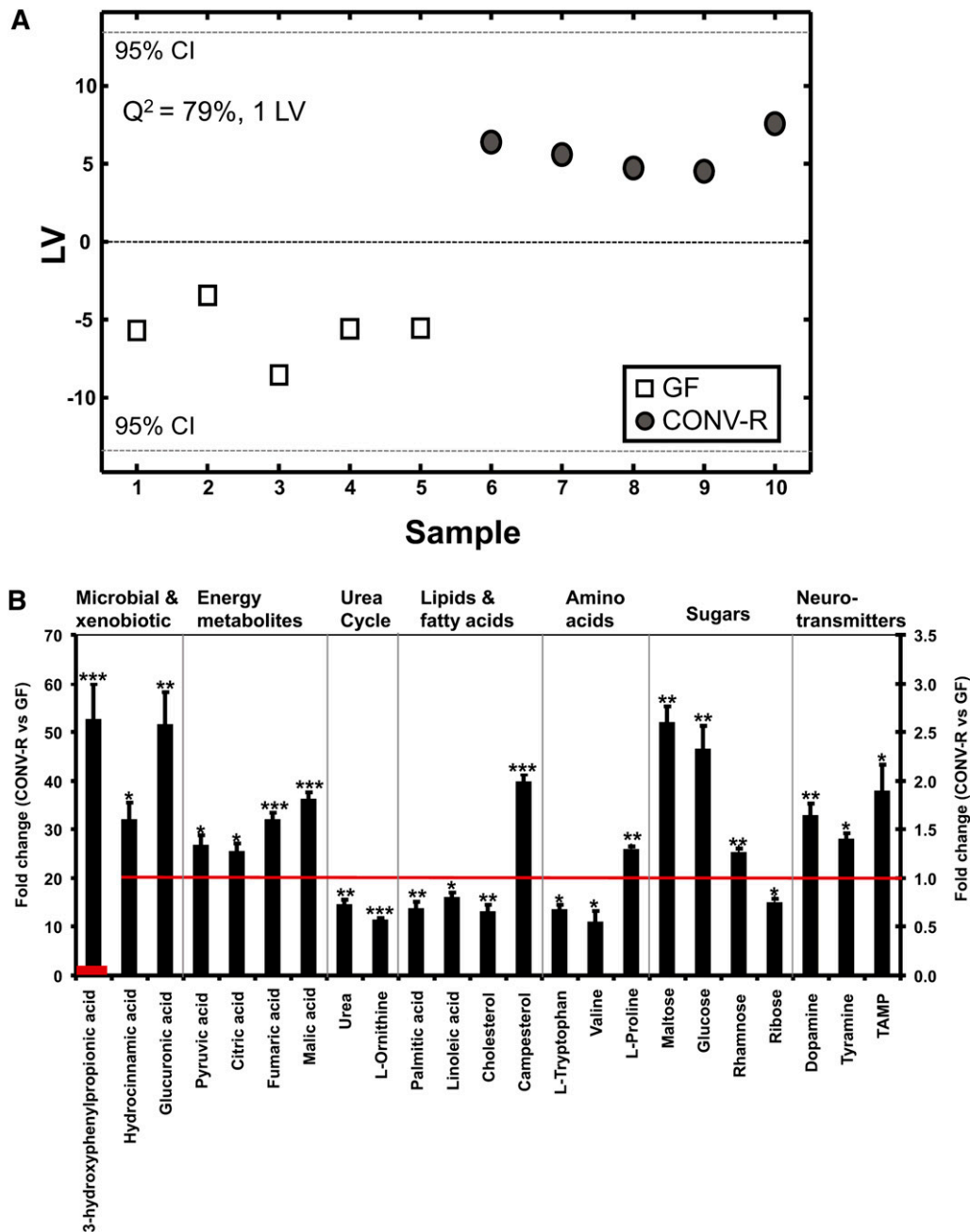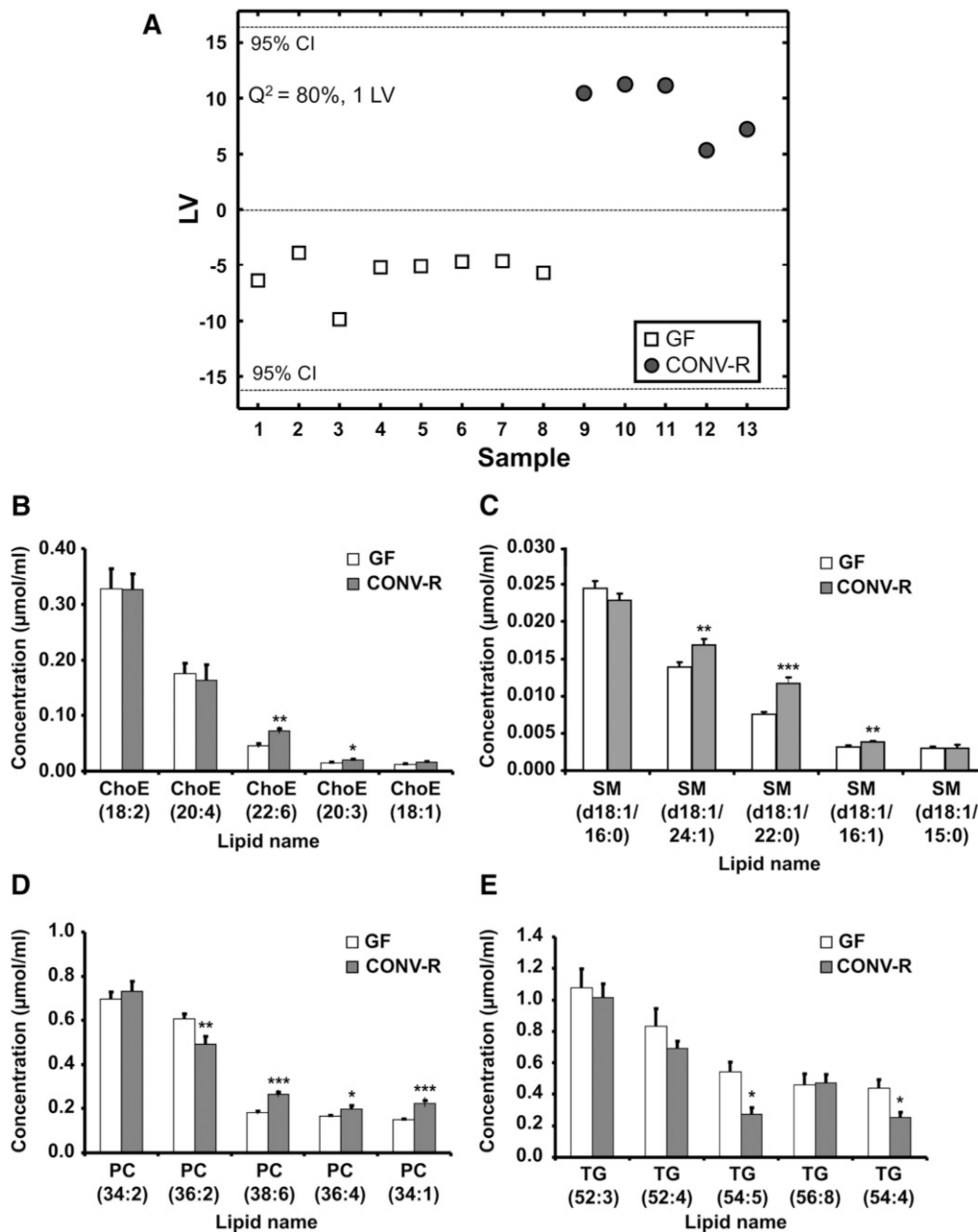
Fig. 1. Serum metabolite profiles in CONV-R compared with GF mice. A: PLS/DA of serum metabolites from GF (n = 5) and CONV-R (n = 5) mice after a 4 h fast. Scores for latent variable LV1 and sample are depicted. Regression coefficients and VIP scores for the top ranked metabolites are listed in supplementary Table I. B: Selected serum metabolites that are significantly different in CONV-R (n = 5) compared with GF (n = 5) mice. For a complete list of microbially altered serum metabolites, see supplementary Table II. Data are expressed as mean values ± SEM. * $P < 0.05$; ** $P < 0.01$; and *** $P < 0.001$ compared with GF mice.

and all significantly altered lipid species are listed in supplementary Table IV).

We found that CONV-R mice had elevated serum levels of two cholesteryl ester and three sphinghomyelin species (Fig. 2B, C; supplementary Table IV). A more dramatic effect of the gut microbiota was observed for phosphatidylcholines and triglycerides: serum levels of 18 phosphatidylcholine species (including three of the most abundant) were increased in CONV-R mice while three species were reduced; and serum levels of nine triglyceride species (in-

cluding two of the five most abundant) were reduced (Fig. 2D, E; supplementary Table IV).

To investigate whether a shorter microbial colonization could induce similar changes in the serum lipidome, we colonized 12-week-old GF mice for 2 weeks (CONV-D) and analyzed their serum lipids on the same platform as above. We found that the reductions in triglyceride levels in CONV-D mice compared with GF counterparts were similar to those observed in CONV-R mice (supplementary Table IV). In contrast, CONV-D mice did not exhibit

Fig. 2. Serum lipidomic profiles in CONV-R compared with GF mice. A: PLS/DA of serum lipids from GF (n = 8) and CONV-R (n = 5) mice after a 4 h fast. Scores for latent variable LV1 and sample are depicted. Regression coefficients and VIP scores for the top ranked lipids are listed in supplementary Table III. B-E: Absolute concentrations of the most abundant cholesteryl esters (ChoE), sphingomyelins (SM), phosphatidylcholines (PC), and triglycerides (TG) in serum from GF and CONV-R mice. For a complete list of microbially altered serum lipids, see supplementary Table IV. Data are expressed as mean values ± SEM. * $P < 0.05$; ** $P < 0.01$; and *** $P < 0.001$ compared with GF mice.

increased serum levels of cholesteryl esters, sphingomyelins, or phosphatidylcholines (supplementary Table IV). In fact, two of the three reduced phosphatidylcholines in CONV-R mice were also reduced in CONV-D mice (supplementary Table IV).

The gut microbiota affects the adipose lipidome

We also explored the effect of the gut microbiota on the adipose lipidome by analyzing epididymal adipose tissue using the same high-resolution lipidomics technique and

mice as above. PLS/DA modeling and clustering revealed significant differences in the global adipose lipid profiles between CONV-R and GF mice after a 4 h fast (**Fig. 3A**; corresponding VIP values are listed in supplementary Table V and significantly altered lipid species are listed in supplementary Table VI).

In contrast to the differences observed in the serum lipidome, the only significant change in the phosphatidylcholine species was a decrease in one of the most abundant species in adipose tissue from CONV-R mice (Fig. 3B) and
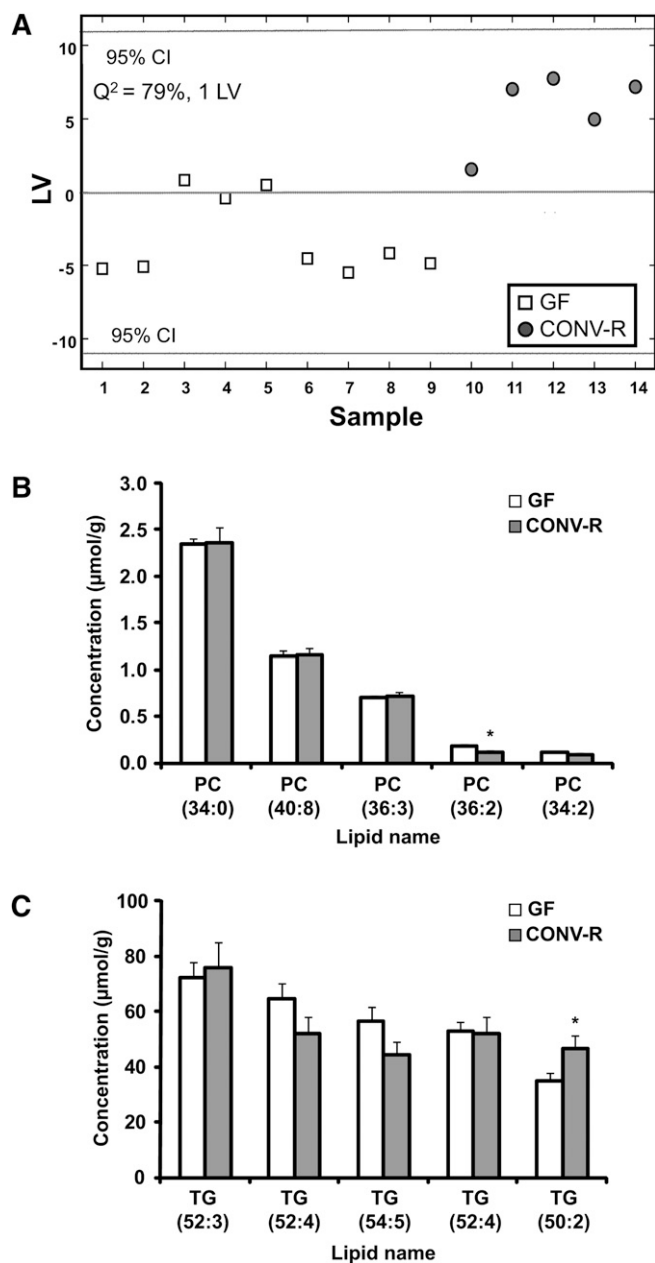
Fig. 3. Lipidomic profiles of epidiymal adipose tissue in CONV-R compared with GF mice. A: PLS/DA of adipose lipids from GF (n = 9) and CONV-R (n = 5) mice after a 4 h fast. Scores for latent variable LV1 and sample are depicted. Regression coefficients and VIP scores for the top ranked lipids are listed in supplementary Table V. B–C: Absolute concentrations of the most abundant phosphatidylcholines (PC) and triglycerides (TG) in adipose tissue from GF and CONV-R mice. For a complete list of microbially altered adipose lipids, see supplementary Table VI. Data are expressed as mean values ± SEM. * *P* < 0.05 compared with GF mice.

there were no alterations in the cholesteryl ester and sphingomyelin species (data not shown). Of all the lipid species measured in the adipose tissue, the gut microbiota had its greatest effect on the triglycerides: in further contrast to the serum lipidome, adipose levels of 13 triglyceride species (including one of the most abundant) were increased in CONV-R mice and only two were reduced (Fig. 3C; supplementary Table VI). As expected the in-

creased triglyceride levels correlated with increased adipose mass and elevated levels of leptin (10.4 ± 1.9 vs. 22.0 ± 1.3 ng/ml, *P* = 0.003, n = 4/group) and insulin (1.3 ± 0.3 vs. 3.8 ± 0.9 ng/ml, *P* = 0.03, n = 4/group) in CONV-R mice compared with GF counterparts, which is agreement with a previous study (16).

The gut microbiota affects the liver lipidome

We next used the same high-resolution lipidomics technique and mice as above to analyze the effect of the gut microbiota on the liver lipidome. PLS/DA modeling and clustering revealed significant differences in the global liver lipid profiles between CONV-R and GF mice after a 4 h fast (**Fig. 4A**, corresponding VIP values are listed in supplementary Table VII and significantly altered lipid species are listed in supplementary Table SVIII).

We observed many more microbiota-related changes in the liver lipidome compared with the serum and adipose tissue (supplementary Table VIII). In contrast to the serum lipidome, we observed decreased levels of two of the three most abundant cholesteryl ester species in CONV-R mice (Fig. 4B). We also observed increases in four of the shorter phosphatidylcholines (≤36C) and decreases in the longer (≥38C) phosphatidylcholines in CONV-R mice (supplementary Table VIII). Furthermore, 95 triglyceride species (including four of the most abundant) increased in CONV-R mice and only two decreased (Fig. 4C; supplementary Table VIII).

In contrast to serum triglycerides, the liver triglycerides only trended toward being increased in CONV-D mice following a 2 week colonization of GF mice (supplementary Table VIII), suggesting that liver triglycerides responded slower than serum triglycerides to colonization.

Levels of chylomicrons but not VLDL are reduced in serum of CONV-R mice

Triglycerides in serum exist mainly packaged in the form of lipoproteins: chylomicrons, which transport dietary triglycerides from the intestine, and VLDL, which transport hepatic triglycerides from the liver to adipose tissue (37). We therefore investigated if a specific effect of the gut microbiota on serum chylomicron levels could explain why we observed reductions in triglyceride species in serum but increases in triglyceride species in adipose tissue and liver from CONV-R mice.

Agarose gel electrophoresis followed by lipid staining of the chylomicron region of agarose gels demonstrated 40% lower chylomicron levels in CONV-R mice compared with GF mice (**Fig. 5A,** B). In contrast, fast protein liquid chromatography followed by enzymatic measurements of triglyceride content in each fraction showed that there were no differences in VLDL-triglyceride levels between CONV-R and GF mice (Fig. 5C). By using Triton WR1339 to inhibit peripheral clearance of lipoproteins, mainly VLDL after an overnight fast, we also showed that the VLDL production rate was higher in CONV-R mice compared with GF mice (Fig. 5E, F).
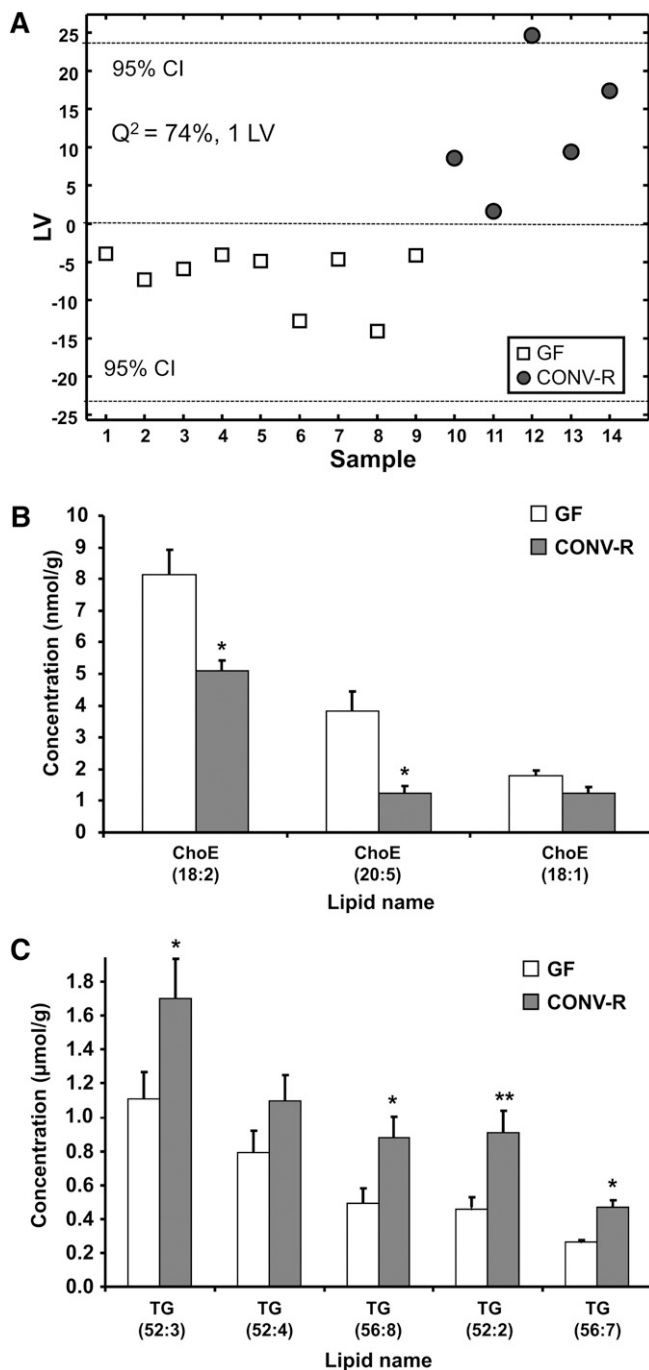
Fig. 4. Lipidomic profiles of liver tissue in CONV-R compared with GF mice. A: PLS/DA of liver lipids from GF (n = 9) and CONV-R (n = 5) mice after a 4 h fast. Scores for latent variable LV1 and sample are depicted. Regression coefficients and VIP scores for the top ranked lipids are listed in supplementary Table VII. B–C: Absolute concentrations of the most abundant cholesteryl esters (ChoE) and triglycerides (TG) in liver tissue from GF and CONV-R mice. For a complete list of microbially altered liver lipids, see supplementary Table VIII. Data are expressed as mean values ± SEM. * $P < 0.05$; ** $P < 0.01$ compared with GF mice.

Because our serum lipidomics data (Fig. 2B) indicated that CONV-R mice had elevated cholesteryl esters, we investigated whether the gut microbiota affected HDL and/or LDL cholesterol. Determining cholesterol levels in the fractions obtained in Fig. 2B suggested that CONV-R mice have slightly elevated LDL cholesterol, while HDL cholesterol was unaltered (Fig. 5D).

### Triglyceride absorption from the gut is not reduced in CONV-R mice

The reduced levels of chylomicrons observed in CONV-R mice after a 4 h fast could be caused by decreased triglyceride absorption from the gut and/or increased triglyceride clearance. To directly test the first possibility, we administered a bolus of heavy whipping cream (36% triglycerides) intragastrically to CONV-R and GF mice after an overnight fast. We did not find any significant differences in serum triglycerides at baseline or after lipid bolus administration (**Fig. 6A**). However, analysis of agarose gels showed that chylomicron levels in serum from CONV-R mice were reduced 4 h after the lipid bolus, but not after 1 h (Fig. 6B). Together, these results are consistent with increased triglyceride clearance but not with decreased triglyceride absorption from the gut in the presence of gut microbiota.

In addition, we performed lipidomics at 1 and 4 h after the lipid bolus to investigate whether the gut microbiota affected the absorption/metabolism of specific lipid species under these conditions. We observed increases in two of the five most abundant phosphatidylcholines in CONV-R mice serum 1 h and 4 h after a lipid bolus and decreases in phosphatidylcholine (36:2) in CONV-R mice serum 1 h after a lipid bolus (supplementary Figs. IB and IIB). The levels of three of the five most abundant sphingomyelins in serum after 4 h and one sphingomyelin after 1 h were elevated in CONV-R mice, and sphingomyelins (d18:1/22:0) were reduced in CONV-R mice serum both 1 h and 4 h after a lipid bolus (supplementary Fig. IB and IIB). All significantly altered lipid species are listed in supplementary Tables IX and X. Our data thus suggest that the gut microbiota does not affect triglyceride absorption; however, other lipid species are modulated by a gut microbiota following lipid administration.

DISCUSSION

In this study, we investigated how the gut microbiota affects host energy and lipid metabolism by comparing serum, white adipose tissue, and liver from CONV-R and GF mice. Analysis of the serum metabolome showed that energy metabolites were increased in CONV-R mice. In addition, we demonstrated that the microbiota modified a number of lipid classes in the serum, adipose tissue, and liver, with its most dramatic effect on triglyceride and phosphatidylcholine species. Our study further supports the emerging view that the gut microbiota plays a role in modulating host metabolism.

Our observation of increased levels of pyruvic acid and tricarboxylic acid metabolites in serum from CONV-R mice is consistent with higher energy metabolism in the presence of gut microbiota (38). In agreement with these findings, we also observed upregulation of genes involved
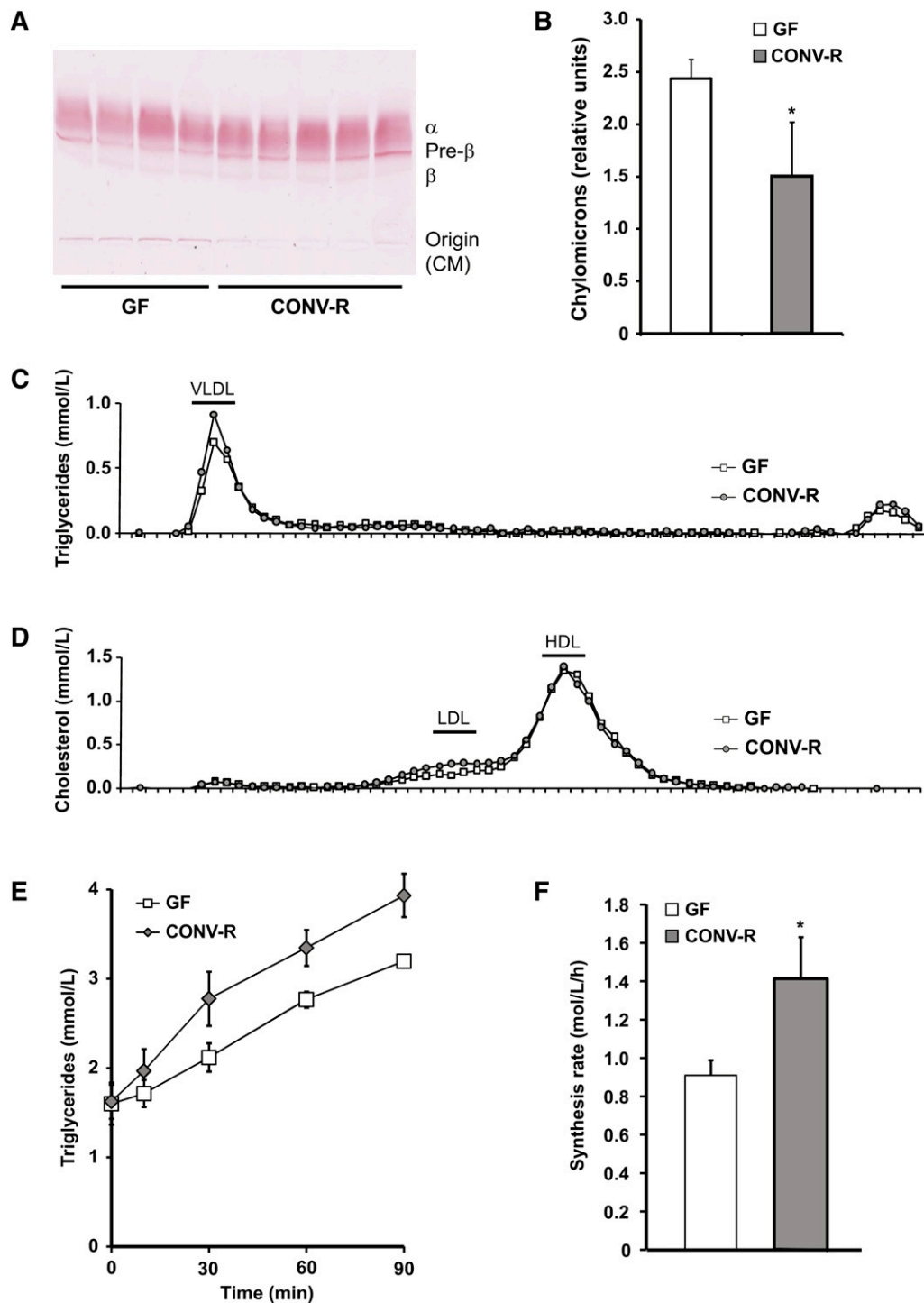
Fig. 5. Serum lipoprotein profiles in CONV-R compared with GF mice. A: Representative agarose gel of the serum samples from GF (n = 4) and CONV-R (n = 5) mice where chylomicrons are at the origin, VLDLs in the preβ band, LDL in the β band, and HDL in the α band. B: Quantification of the agarose gels in (*A*). C: Total triglycerides measured in gel chromatography fractions of pooled serum (n = 5 per group) from GF and CONV-R mice after a 4 h fast. Fractions containing VLDL are indicated. D: Total cholesterol measured in the same gel chromatography fractions as in C. Fractions containing LDL and HDL are indicated. E: Triglycerides in serum from GF (n = 6) and CONV-R (n = 5) mice after an overnight fast and administration of Triton WR 1339. F: VLDL production rates based on data in E. Data are expressed as mean values ± SEM. * $P < 0.05$ compared with GF mice.

in the tricarboxylic acid cycle and pyruvate metabolism in the liver transcriptome of CONV-R versus GF mice (R. Hezaveh, C. Reigstad, P. Gopalacharyulu, M. Oresic, and F. Bäckhed, unpublished data). Furthermore, a recent study of obese and lean twins showed that the gut microbiome (collection of all microbial genes) of obese individuals is associated with an enrichment in carbohydrate and lipid utilizing genes (13). Thus, rapid processing of
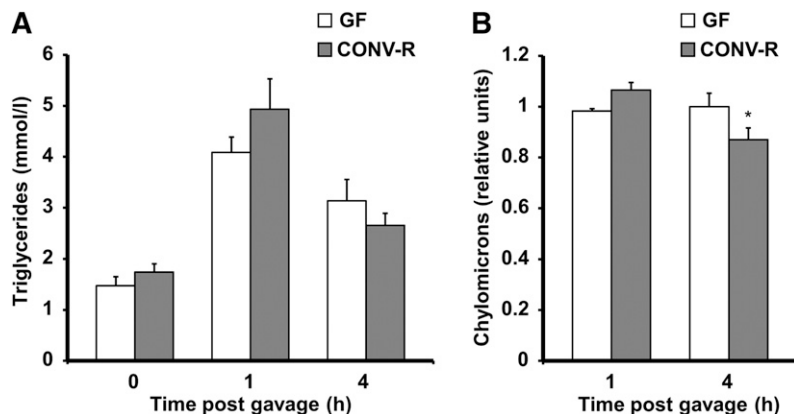
Fig. 6. Postprandial lipid uptake in CONV-R and GF mice. A: Serum triglyceride levels in GF (n = 7–8/time point) and CONV-R (n = 6/time point) before and 1 and 4 h after an intragastric cream (36% fat) bolus. B: Levels of chylomicron remnant levels in the same serum as in A analyzed by agarose gel electrophoresis. * $P < 0.05$ compared with GF mice.

energy metabolites in the liver and other peripheral organs may reflect increased energy availability.

We showed that the microbiota had a dramatic effect on triglyceride species, with reductions in the levels of nine species in serum and increases in 13 species in adipose tissue and 95 species in liver from CONV-R mice compared with GF mice after a 4 h fast. Previous studies have shown reduced triglyceride serum levels and increased liver triglyceride levels and adiposity in the presence of a gut microbiota (16, 17), but this is the first study to highlight the dramatic changes in a large number of individual triglyceride species. We also demonstrated that the increased adiposity results from increased triglycerides and not from

changes in any other lipid species. Interestingly, the increased triglyceride species in adipose tissue from CONV-R mice contained even-numbered fatty acids, indicating that they are derived from de novo lipogenesis (C16), elongation (C18), and desaturation (18:1) (39). In contrast, the two decreased species contained 45 and 53 carbons, respectively, suggesting that they may be derived from the diet. We noted the most extensive microbially induced alterations of triglycerides in the liver, which potentially can be explained by increased substrate influx in the form of short-chain fatty acids from the colon (40) and increased glucose and insulin levels (16). Although we did not directly attempt to address whether microbial colonization
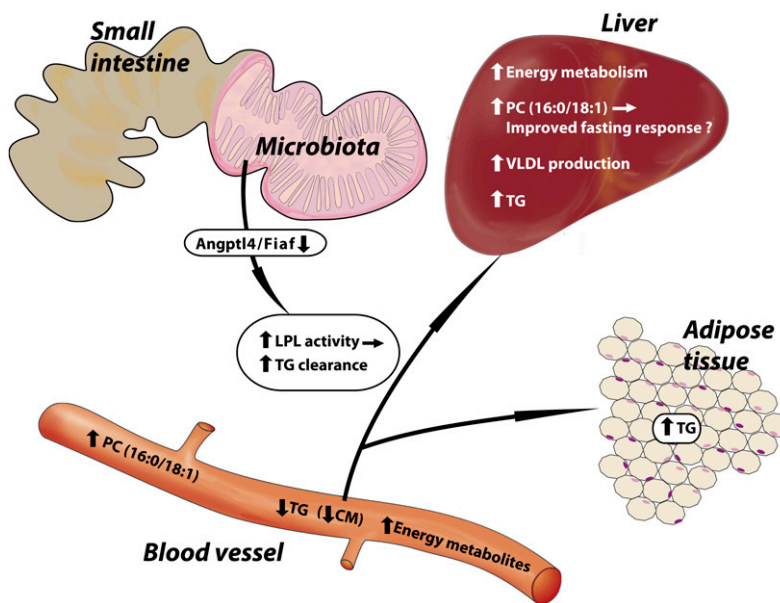
Fig. 7. Summary of the microbiota-induced changes in energy and lipid metabolism identified in our study. Energy metabolites are increased in the serum and are reflected by an upregulation of related genes in the liver transcriptome. Triglyceride (TG) levels are decreased in the serum and increased in adipose tissue and the liver of CONV-R mice after a 4 h fast. The serum reduction in TG is caused by a decrease in chylomicrons (CM). Lipid absorption is not reduced in CONV-R mice, and we propose that lipid clearance is increased. In agreement, we have previously shown that a microbiota increases suppression of angiopoietin-like protein 4/fasting-induced adipose factor (Angptl4/Fiaf) (16), an inhibitor of LPL, which will promote increased lipid clearance. VLDL production in the liver is increased in CONV-R mice, which may explain why VLDL-TG serum levels are not reduced in CONV-R mice despite increased clearance. Furthermore, phosphatidylcholine (16:0/18:1), which has been identified as a potent endogenous PPARα ligand, is increased in the serum and liver of CONV-R mice. Increased activation of PPARα may promote increased lipid clearance by inducing expression of LPL.

affected the subcellular compartmentalization of triglycerides, a previous study suggested that increased triglycerides accumulate lipid droplets (16).

Conventionalization of GF mice with a normal microbiota for 14 days resulted in a shift in the levels of serum triglyceride species similar to that observed in CONV-R mice but did not alter the serum levels of cholesteryl esters, sphingomyelins, and phosphatidylcholines compared with GF mice. Although the mechanism at present is unclear, the shift in triglycerides tended to be more dramatic in CONV-D mice. In contrast, a 14-day colonization did not alter triglyceride in the liver as dramatically. Thus, serum and liver display different kinetics in response to conventionalization. We have previously shown that mice that have been conventionalized for 14 days have the same microbial composition as the inoculating microbiota (16), and it is thus unlikely that the lack of effect on lipids other than triglycerides was caused by incomplete colonization. Although further work is required to determine the implication of this result, it is possible that the gut microbiota has a more immediate effect on molecules involved in energy storage than on structural and signaling molecules.

We showed that the presence of a gut microbiota reduced serum levels of chylomicrons but not VLDL-triglycerides after a 4 h fast. We then investigated if the reduction in chylomicrons resulted from decreased lipid absorption from the gut and/or increased lipid clearance. Because it is known that the gut microbiota promotes deconjugation of bile acids in the intestine (41), resulting in less efficient emulsification of dietary lipids (42), we expected to observe reduced triglyceride absorption from the gut. Surprisingly, we did not observe significant differences in triglyceride absorption between CONV-R and GF mice after administration of a triglyceride bolus. However, we did see differences in some phosphatidylcholines and sphingomyelins. It should be noted that the gut microbiota is known to increase gastrointestinal motility (43), which potentially could mask decreased absorptive capacity in CONV-R mice.

Although serum triglyceride levels were not affected by the presence of the gut microbiota 4 h after a lipid bolus, the serum chylomicron levels were reduced, consistent with increased lipid clearance. Indeed, we have earlier shown that conventionalization of GF mice suppresses an inhibitor of LPL (16). Increased activation of LPL will promote increased lipid clearance, resulting in reduced serum triglyceride levels together with increased storage of lipids in adipose tissue and the liver, as observed in the CONV-R mice in our study. Furthermore, we also showed that the VLDL production rate increased in CONV-R mice. Increased VLDL production may explain why we did not observe altered VLDL-triglyceride levels in CONV-R mice despite increased lipid clearance.

We also observed that the gut microbiota has a major influence on phosphatidylcholine species, with increases in the levels of 16 species in serum and 4 shorter chain species in the liver, and decreases in 1 species in adipose tissue and 4 longer chain species in liver from CONV-R mice compared with GF mice after a 4 h fast. Phosphatidylcholines are a major component of biological membranes. They provide a structural framework, maintain membrane permeability and also play a role in membrane-mediated cell signaling (44). Circulating phosphatidylcholines are incorporated into lipoprotein particles (45) and are a major source of choline in the body. Phosphatidylcholines can either be derived from the diet or from de novo synthesis in the liver (45), but it is not clear whether the gut microbiota increases intestinal absorption and/or hepatic biosynthesis.

Of particular interest, we found increased levels of phosphatidylcholine (34:1, identified as 16:0/18:1 by tandem MS, as shown in supplementary Fig. III) in both serum and liver tissue of CONV-R mice. This species is a common phosphatidylcholine in the liver and comprises approximately 11% of the nuclear phosphatidylcholines (46). A recent study showed that phosphatidylcholine (16:0/18:1) is a physiologic agonist of the nuclear receptor peroxisome proliferator-activated receptor (PPAR)α (46), which promotes fatty acid oxidation, lipid transport, ketogenesis, and gluconeogenesis, and induces expression of LPL (47). Here, we propose that the microbiota-induced increases in phosphatidylcholine (16:0/18:1) observed in serum and liver may potentially play a role in increased triglyceride clearance in CONV-R mice through increased PPARα-mediated activation of LPL.

CONV-R mice die less rapidly in response to starvation compared with their GF counterparts, despite losing weight at approximately the same rate (48). One possible explanation is that the gut microbiota is essential to promote PPARα-regulated increases in hepatic production of ketone bodies in the fasting state (49). Although it remains to be shown if this response is mediated by phosphatidylcholine (16:0/18:1), it further demonstrates the intricate role of the gut microbiota in modulating energy metabolism.

A large-scale metabolomic study in a birth cohort of 8,026 children at genetic risk of type 1 diabetes (T1D) showed that cord serum as well as prospective serum metabolic profiles of children who later progressed to T1D were characterized by low levels of phosphatidylcholines and tricarboxylic acid cycle metabolites (50). The observed profiles in T1D progressors are thus similar to those of GF mice in the present study. It would therefore be of interest to analyze the gut microbiota in the children who progress to T1D to determine if this can identify any deficiency or impaired function that predisposes them to the disease.

The gut microbiota has coevolved with its host and provides the host with traits that we did not have to evolve on our own. Here, we demonstrate that the gut microbiota increases energy metabolism and has systemic effects on host lipid metabolism, especially triglycerides and phosphatidylcholines (**Fig. 7**). Thus, the gut microbiota affects both energy storing and signaling lipids, reinforcing its role as an important environmental factor that regulates host metabolism and promotes obesity and diabetes.

REFERENCES

1. Eckburg, P. B., E. M. Bik, C. N. Bernstein, E. Purdom, L. Dethlefsen, M. Sargent, S. R. Gill, K. E. Nelson, and D. A. Relman. 2005. Diversity of the human intestinal microbial flora. *Science.* **308:** 1635–1638.

2. Ley, R. E., F. Backhed, P. Turnbaugh, C. A. Lozupone, R. D. Knight, and J. I. Gordon. 2005. Obesity alters gut microbial ecology. *Proc. Natl. Acad. Sci. USA.* **102:** 11070–11075.

3. Ley, R. E., P. J. Turnbaugh, S. Klein, and J. I. Gordon. 2006. Microbial ecology: human gut microbes associated with obesity. *Nature.* **444:** 1022–1023.

4. Dethlefsen, L., S. Huse, M. L. Sogin, and D. A. Relman. 2008. The pervasive effects of an antibiotic on the human gut microbiota, as revealed by deep 16S rRNA sequencing. *PLoS Biol.* **6:** e280.

5. Ley, R. E., M. Hamady, C. Lozupone, P. J. Turnbaugh, R. R. Ramey, J. S. Bircher, M. L. Schlegel, T. A. Tucker, M. D. Schrenzel, R. Knight, et al. 2008. Evolution of mammals and their gut microbes. *Science.* **320:** 1647–1651.

6. Hooper, L. V., M. H. Wong, A. Thelin, L. Hansson, P. G. Falk, and J. I. Gordon. 2001. Molecular analysis of commensal host-microbial relationships in the intestine. *Science.* **291:** 881–884.

7. Rawls, J. F., M. A. Mahowald, R. E. Ley, and J. I. Gordon. 2006. Reciprocal gut microbiota transplants from zebrafish and mice to germ-free recipients reveal host habitat selection. *Cell.* **127:** 423–433.

8. Li, M., B. Wang, M. Zhang, M. Rantalainen, S. Wang, H. Zhou, Y. Zhang, J. Shen, X. Pang, H. Wei, et al. 2008. Symbiotic gut microbes modulate human metabolic phenotypes. *Proc. Natl. Acad. Sci. USA.* **105:** 2117–2122.

9. Hooper, L. V., T. Midtvedt, and J. I. Gordon. 2002. How host-microbial interactions shape the nutrient environment of the mammalian intestine. *Annu. Rev. Nutr.* **22:** 283–307.

10. O'Hara A. M., and F. Shanahan. 2006. The gut flora as a forgotten organ. *EMBO Rep.* **7:** 688–693.

11. Bäckhed, F., R. E. Ley, J. L. Sonnenburg, D. A. Peterson, and J. I. Gordon. 2005. Host-bacterial mutualism in the human intestine. *Science.* **307:** 1915–1920.

12. Smith, K., K. D. McCoy, and A. J. Macpherson. 2007. Use of axenic animals in studying the adaptation of mammals to their commensal intestinal microbiota. *Semin. Immunol.* **19:** 59–69.

13. Turnbaugh, P. J., M. Hamady, T. Yatsunenko, B. L. Cantarel, A. Duncan, R. E. Ley, M. L. Sogin, W. J. Jones, B. A. Roe, J. P. Affourtit, et al. 2009. A core gut microbiome in obese and lean twins. *Nature.* **457:** 480–484.

14. Turnbaugh, P. J., F. Backhed, L. Fulton, and J. I. Gordon. 2008. Diet-induced obesity is linked to marked but reversible alterations in the mouse distal gut microbiome. *Cell Host Microbe.* **3:** 213–223.

15. Turnbaugh, P. J., R. E. Ley, M. A. Mahowald, V. Magrini, E. R. Mardis, and J. I. Gordon. 2006. An obesity-associated gut microbiome with increased capacity for energy harvest. *Nature.* **444:** 1027–1031.

16. Bäckhed, F., H. Ding, T. Wang, L. V. Hooper, G. Y. Koh, A. Nagy, C. F. Semenkovich, and J. I. Gordon. 2004. The gut microbiota as an environmental factor that regulates fat storage. *Proc. Natl. Acad. Sci. USA.* **101:** 15718–15723.

17. Bäckhed, F., J. K. Manchester, C. F. Semenkovich, and J. I. Gordon. 2007. Mechanisms underlying the resistance to diet-induced obesity in germ-free mice. *Proc. Natl. Acad. Sci. USA.* **104:** 979–984.

18. Claus, S. P., T. M. Tsang, Y. Wang, O. Cloarec, E. Skordi, F-P. Martin, S. Rezzi, A. Ross, S. Kochhar, E. Holmes, et al. 2008. Systemic multicompartmental effects of the gut microbiome on mouse metabolic phenotypes. *Mol. Syst. Biol.* **4:** 219.

19. Wikoff, W. R., A. T. Anfora, J. Liu, P. G. Schultz, S. A. Lesley, E. C. Peters, and G. Siuzdak. 2009. Metabolomics analysis reveals large effects of gut microflora on mammalian blood metabolites. *Proc. Natl. Acad. Sci. USA.* **106:** 3698–3703.

20. Martin, F. P., M. E. Dumas, Y. Wang, C. Legido-Quigley, I. K. Yap, H. Tang, S. Zirah, G. M. Murphy, O. Cloarec, J. C. Lindon, et al. 2007. A top-down systems biology view of microbiome-mammalian metabolic interactions in a mouse model. *Mol. Syst. Biol.* **3:** 112.

21. Martin, F. P., Y. Wang, N. Sprenger, I. K. Yap, T. Lundstedt, P. Lek, S. Rezzi, Z. Ramadan, P. van Bladeren, L. B. Fay, et al. 2008. Probiotic modulation of symbiotic gut microbial-host metabolic interactions in a humanized microbiome mouse model. *Mol. Syst. Biol.* **4:** 157.

22. Martin, F. P., Y. Wang, N. Sprenger, I. K. Yap, S. Rezzi, Z. Ramadan, E. Pere-Trepat, F. Rochat, C. Cherbut, P. van Bladeren, et al. 2008. Top-down systems biology integration of conditional prebiotic modulated transgenomic interactions in a humanized microbiome mouse model. *Mol. Syst. Biol.* **4:** 205.

23. Smith, L. C., H. J. Pownall, and A. M. Gotto. 1978. The plasma lipoproteins: structure and metabolism. *Annu. Rev. Biochem.* **47:** 751–777.

24. Laaksonen, R., M. Katajamaa, H. Paiva, M. Sysi-Aho, L. Saarinen, P. Junni, D. Lutjohann, J. Smet, R. Van Coster, T. Seppanen-Laakso, et al. 2006. A systems biology strategy reveals biological pathways and plasma biomarker candidates for potentially toxic statin-induced changes in muscle. *PLoS One.* **1:** e97.

25. Geladi, P., and B. R. Kowalski. 1986. Partial least-squares regression: a tutorial. *Anal. Chim. Acta.* **185:** 1–17.

26. Barker, M., and W. Rayens. 2003. Partial least squares for discrimination. *J. Chemometr.* **17:** 166–173.

27. de Jong, S. 1993. SIMPLS: an alternative approach to partial least squares regression. *Chemom. Intell. Lab. Syst.* **18:** 251–263.

28. Pears, M. R., J. D. Cooper, H. M. Mitchison, R. J. Mortishire-Smith, D. A. Pearce, and J. L. Griffin. 2005. High resolution 1H NMR-based metabolomics indicates a neurotransmitter cycling deficit in cerebral tissue from a mouse model of Batten Disease. *J. Biol. Chem.* **280:** 42508–42514.

29. Brindle, J. T., H. Antti, E. Holmes, G. Tranter, J. K. Nicholson, H. W. L. Bethell, S. Clarke, P. M. Schofield, E. McKilligin, D. E. Mosedale, et al. 2002. Rapid and noninvasive diagnosis of the presence and severity of coronary heart disease using 1H-NMR-based metabonomics. *Nat. Med.* **8:** 1439–1445.

30. Wise, B. M., N. B. Gallagher, R. Bro, J. M. Shaver, W. Windig, and J. S. Koch. 2006. PLS Toolbox 4.0 for Use with Matlab. Eigenvector Research Inc., Manson, WA.

31. Young, S. G., S. J. Bertics, L. K. Curtiss, and J. L. Witztum. 1987. Characterization of an abnormal species of apolipoprotein B, apolipoprotein B-37, associated with familial hypobetalipoproteinemia. *J. Clin. Invest.* **79:** 1831–1841.

32. Benjamini, Y., D. Drai, G. Elmer, N. Kafkafi, and I. Golani. 2001. Controlling the false discovery rate in behavior genetics research. *Behav. Brain Res.* **125:** 279–284.

33. Bazzocco, S., I. Mattila, S. Guyot, C. Renard, and A-M. Aura. 2008. Factors affecting the conversion of apple polyphenols to phenolic acids and fruit matrix to short-chain fatty acids by human faecal microbiota in vitro. *Eur. J. Nutr.* **47:** 442–452.

34. Moss, C. W., M. A. Lambert, and D. J. Goldsmith. 1970. Production of hydrocinnamic acid by clostridia. *Appl. Microbiol.* **19:** 375–378.

35. Tashjian, A. H., Jr., E. J. Armstrong, J. N. Galanter, A. W. Armstrong, R. A. Arnaout, and H. S. Rose. 2005. Pharmacology of the bacterial cell wall. *In* Principles of Pharmacology: The Pathophysiologic Basis of Drug Therapy. D. E. Golan, editor. Lippincott Williams and Wilkins, Baltimore. 569.

36. Tukey, R. H., and C. P. Strassburg. 2000. Human UDP-glucuronosyltransferases: metabolism, expression, and disease. *Annu. Rev. Pharmacol. Toxicol.* **40:** 581–616.

37. Olofsson, S. O., L. Asp, and J. Boren. 1999. The assembly and secretion of apolipoprotein B-containing lipoproteins. *Curr. Opin. Lipidol.* **10:** 341–346.

38. Wostmann, B. S., C. Larkin, A. Moriarty, and E. Bruckner-Kardoss. 1983. Dietary intake, energy metabolism, and excretory losses of adult male germfree Wistar rats. *Lab. Anim. Sci.* **33:** 46–50.

39. Postic, C., and J. Girard. 2008. Contribution of de novo fatty acid synthesis to hepatic steatosis and insulin resistance: lessons from genetically engineered mice. *J. Clin. Invest.* **118:** 829–838.

40. Bergman, E. N. 1990. Energy contributions of volatile fatty acids from the gastrointestinal tract in various species. *Physiol. Rev.* **70:** 567–590.

41. Midtvedt, T. 1974. Microbial bile acid transformation. *Am. J. Clin. Nutr.* **27:** 1341–1347.

42. Armstrong, M. J., and M. C. Carey. 1982. The hydrophobic-hydrophilic balance of bile salts. Inverse correlation between reverse-phase high performance liquid chromatographic mobilities and micellar cholesterol-solubilizing capacities. *J. Lipid Res.* **23:** 70–80.

43. Abrams, G. D., and J. E. Bishop. 1967. Effect of the normal microbial flora on gastrointestinal motility. *Proc. Soc. Exp. Biol. Med.* **126:** 301–304.

44. Exton, J. H. 1990. Signaling through phosphatidylcholine breakdown. *J. Biol. Chem.* **265:** 1–4.

45. Vance, D. E. 2008. Role of phosphatidylcholine biosynthesis in the regulation of lipoprotein homeostasis. *Curr. Opin. Lipidol.* **19:** 229–234.

46. Chakravarthy, M. V., I. J. Lodhi, L. Yin, R. R. Malapaka, H. E. Xu, J. Turk, and C. F. Semenkovich. 2009. Identification of a physiologically relevant endogenous ligand for PPARalpha in liver. *Cell.* **138:** 476–488.

47. Reddy, J. K., and T. Hashimoto. 2001. Peroxisomal beta-oxidation and peroxisome proliferator-activated receptor alpha: an adaptive metabolic system. *Annu. Rev. Nutr.* **21:** 193–230.

48. Tennant, B., O. J. Malm, R. E. Horowitz, and S. M. Levenson. 1968. Response of germfree, conventional, conventionalized and E. coli monocontaminated mice to starvation. *J. Nutr.* **94:** 151–160.

49. Crawford, P. A., J. R. Crowley, N. Sambandam, B. D. Muegge, E. K. Costello, M. Hamady, R. Knight, and J. I. Gordon. 2009. Regulation of myocardial ketone body metabolism by the gut microbiota during nutrient deprivation. *Proc. Natl. Acad. Sci. USA.* **106:** 11276–11281.

50. Oresic, M., S. Simell, M. Sysi-Aho, K. Nanto-Salonen, T. Seppanen-Laakso, V. Parikka, M. Katajamaa, A. Hekkala, I. Mattila, P. Keskinen, et al. 2008. Dysregulation of lipid and amino acid metabolism precedes islet autoimmunity in children who later progress to type 1 diabetes. *J. Exp. Med.* **205:** 2975–2984.